REPORT DOCUMENTATION PAGE

Public reporting burden for this collection of information is estimated to average 1 hour per response, including the time for reviewing instructions, searching existing data sources, gathering and maintaining the data needed, and completing and reviewing the collection of information. Send comments regarding this burden estimate or any other aspect of this collection of information, including suggestions for reducing this burden, to Washington Headquarters Services, Directorate for Information Operations and Reports, 1215 Jefferson Davis Highway, Suite 1204, Arlington, VA 22202-4302, and to the Office of Management and Budget, Paperwork Reduction Project (0704-0188), Washington, DC 20503.

1. AGENCY USE ONLY (Leave blank)	2. REPORT DATE August 2001	3. REPORT TYPE AND DATES COVERED Conference Paper 1 October 2000 – 6 August 2001

4. TITLE AND SUBTITLE	5. FUNDING NUMBERS
Nonlinear, Hybrid Bank-To-Turn/Skid-To-Turn Missile Autopilot Design	Contract #: JON: 2304AW10 PE: 61102F PR: 2304 TA: AW WU: 10

6. AUTHOR(S)
James R. Cloutier[1] and Donald T. Stansbery[2]

7. PERFORMING ORGANIZATION NAME(S) AND ADDRESS(ES)	8. PERFORMING ORGANIZATION REPORT NUMBER
[1]Air Force Research Laboratory [2]CACI/TEAS Group Munitions Directorate 101 W. Eglin Blvd AFRL/MNGN Suite 341 101 W. Eglin Blvd Ste 341 Eglin AFB, FL 32542-6810 Eglin AFB, FL 32542-6810	

9. SPONSORING/MONITORING AGENCY NAME(S) AND ADDRESS(ES)	10. SPONSORING/MONITORING AGENCY REPORT NUMBER
Dr. Belinda King AFRL/AFOSR/NM 801 North Randolph St. Rm 732 Arlington, VA 22203-1977	N/A

11. SUPPLEMENTARY NOTES

12a. DISTRIBUTION/AVAILABILITY STATEMENT	12b. DISTRIBUTION CODE
DISTRIBUTION A: Approved for public release; distribution unlimited	

13. ABSTRACT: A full-envelope, hybrid bank-to-turn (BTT)/ skid-to-turn (STT) autopilot design for an air-breathing air-to-air missile is carried out using the state-dependent Riccati equation (SDRE) technique of nonlinear control. Hybrid BTT/STT autopilot command logic is used to convert the guidance law's commanded acceleration to angle of attack, side-slip, and bank angle reference commands for the autopilot. In the midcourse and terminal phases of flight, BTT control is employed to prevent engine flameout. In the endgame, STT control is employed to increase response time. As the missile approaches the endgame phase and passes a preset time-to-go threshold, STT commands are ramped into the BTT commands over a preselected time interval to attenuate transient responses. During this interval, the missile is flying hybrid BTT/STT. An SDRE nonlinear outer-loop controller converts the angle-of-attack, sideslip, and bank angle commands to body rates commands for the inner loop. An inner-loop SDRE nonlinear controller converts the body rate commands to fin commands. Hard bounds on the fin deflections are embedded within the inner-loop controller dynamics ensuring that the autopilot only commands deflections that are achievable. The nonlinear design is evaluated using a detailed six-degrees-of-freedom simulation

14. SUBJECT TERM	15. NUMBER OF PAGES
State-Dependent Riccati Equations, Missile Autopilot Design Methodology	11
	16. PRICE CODE

17. SECURITY CLASSIFICATION OF REPORT	18. SECURITY CLASSIFICATION OF THIS PAGE	19. SECURITY CLASSIFICATION OF ABSTRACT	20. LIMITATION OF ABSTRACT
UNCLASSIFIED	UNCLASSIFIED	UNCLASSIFIED	UL

20020528 045

Nonlinear, Hybrid Bank-to-Turn/Skid-to-Turn Missile Autopilot Design

James R. Cloutier*
U.S. Air Force Research Laboratory
Munitions Directorate
101 W. Eglin Blvd., Ste. 341
Eglin AFB, FL 32542-6810
email: james.cloutier@eglin.af.mil

Donald T. Stansbery[†]
CACI/TEAS Group
214 Government St.
Niceville, FL 32578
email: stansbed@eglin.af.mil

Abstract

A full-envelope, hybrid bank-to-turn (BTT)/ skid-to-turn (STT) autopilot design for an air-breathing air-to-air missile is carried out using the state-dependent Riccati equation (SDRE) technique of nonlinear control. Hybrid BTT/STT autopilot command logic is used to convert the guidance law's commanded acceleration to angle of attack, side-slip, and bank angle reference commands for the autopilot. In the midcourse and terminal phases of flight, BTT control is employed to prevent engine flameout. In the endgame, STT control is employed to increase response time. As the missile approaches the endgame phase and passes a preset time-to-go threshold, STT commands are ramped into the BTT commands over a preselected time interval to attenuate transient responses. During this interval, the missile is flying hybrid BTT/STT.

An SDRE nonlinear outer-loop controller converts the angle-of-attack, sideslip, and bank angle commands to body rates commands for the inner loop. An inner-loop SDRE nonlinear controller converts the body rate commands to fin commands. Hard bounds on the fin deflections are embedded within the inner-loop controller dynamics ensuring that the autopilot only commands deflections that are achievable. The nonlinear design is evaluated using a detailed six-degrees-of-freedom simulation.

Nomenclature

u, v, w	body-frame velocity components
V	missile speed
$\mathcal{M}$	Mach
α	angle of attack
β	angle of sideslip
μ	bank angle about the velocity vector
γ	vertical flight-path angle
p, q, r	body-frame roll, pitch, and yaw rates
ψ, θ, ϕ	Euler yaw, pitch, and roll angles
S	reference area
d	reference length
M	missile mass
$\bar{q}$	dynamic pressure
h	altitude
g	gravity
T	thrust
$\delta p, \delta q, \delta r$	aileron, elevator, and rudder fin deflections
I_x, I_y, I_z	moments of inertia about body-frame x, y, z-axes
C_A	axial force coefficient
C_Y	side force coefficient
C_N	normal force coefficient
C_l	rolling moment coefficient
C_m	pitching moment coefficient
C_n	yawing moment coefficient
C_{i_j}	aerodynamic force or moment derivative i with respect to state or input j

---

*Associate Fellow AIAA
[†]Senior Member AIAA

1. Introduction

In order to achieve adequate performance over the entire envelope of operating conditions, the autopilot of a modern air-to-air tactical missile must be nonlinear. The nonlinearity arises either through the gain-scheduling of linear point designs [1, 2, 3, 4] or through the direct application of a nonlinear control technique to the problem. Nonlinear control methods which have been used for missile autopilot design include recursive backstepping [5], dynamic inversion [6, 7], sliding mode control [8], neural networks [9], linear parameter varying (LPV) control [10, 11], and state-dependent Riccati equation (SDRE) techniques [12, 13, 14]. In [12], the SDRE H_2 method was used to design a full-envelope pitch autopilot. The SDRE H_2 design has the same structure as a linear H_2 design with all of the coefficient matrices being state-dependent. In [13, 14], the SDRE method of nonlinear regulation and the differential SDRE method were used, respectively, to develop integrated guidance/autopilot designs. The differential SDRE method has the same structure as the time-varying finite-horizon linear quadratic regulator (LQR) with all of the coefficient matrices being state-dependent and requires the solution of a state-dependent differential Riccati equation.

In this paper, we use the algebraic SDRE method of nonlinear regulation to design a hybrid bank-to-turn (BTT)/ skid-to-turn (STT) autopilot for the control of an air-breathing air-to-air missile. BTT is used in the midcourse and terminal phases to prevent engine flameout. STT is used in the endgame to increase response time. To attenuate transient responses, the STT command logic is ramped into the BTT command logic as the missile transitions from the terminal phase to the endgame.

The system dynamics are presented in the next section. An overview of the SDRE technique with integral servomechanism action is given in Section 3. The SDRE outer-loop and inner-loop designs are carried out in Section 4. The BBT/STT command logic is described in Section 5. Design results evaluated in a detailed six-degrees-of-freedom simulation are presented in Section 6. The paper is then closed with a Summary section.

2. System Dynamics

The system dynamics for a generic air-to-air missile with the aerodynamic model and database generated in [15] are given below in terms of the missile's speed, angle of attack, sideslip, bank angle, roll rate, pitch rate, and yaw rate:

$$\dot{V} = -\frac{\bar{q}S}{M}C_A \cos\alpha\cos\beta + \frac{\bar{q}S}{M}C_{Y_0}\sin\beta - \frac{\bar{q}S}{M}C_{N_0}\sin\alpha\cos\beta - g\sin\gamma$$
$$+\frac{\cos\alpha\cos\beta}{M}T + \frac{\bar{q}S}{M}[(C_{Y_{\delta p}}\sin\beta - C_{N_{\delta p}}\sin\alpha\cos\beta)\delta p - (C_{Y_{\delta q}}\sin\beta$$
$$-C_{N_{\delta q}}\sin\alpha\cos\beta)\delta q - (C_{Y_{\delta r}}\sin\beta - C_{N_{\delta r}}\sin\alpha\cos\beta)\delta r] \quad (1)$$

$$\dot{\alpha} = q - \tan\beta\cos\alpha p - \tan\beta\sin\alpha r + \frac{g}{V\cos\beta}\cos\gamma\cos\mu$$
$$-\frac{\bar{q}S}{MV\cos\beta}C_{N_0}\cos\alpha + \frac{\bar{q}S}{MV\cos\beta}C_A\sin\alpha - \frac{\sin\alpha}{MV\cos\beta}T$$
$$-\frac{\bar{q}S\cos\alpha}{MV\cos\beta}(C_{N_{\delta p}}\delta p - C_{N_{\delta q}}\delta q - C_{N_{\delta r}}\delta r) \quad (2)$$

$$\dot{\beta} = \sin\alpha p - \cos\alpha r + \frac{g}{V}\cos\gamma\sin\mu + \frac{\bar{q}S}{MV}C_{N_0}\sin\alpha\sin\beta$$
$$+\frac{\bar{q}S}{MV}C_A\cos\alpha\sin\beta + \frac{\bar{q}S}{MV}C_{Y_0}\cos\beta - \frac{\cos\alpha\sin\beta}{MV}T + \frac{\bar{q}S}{MV}[(C_{Y_{\delta p}}\cos\beta$$
$$+C_{N_{\delta p}}\sin\alpha\sin\beta)\delta p - (C_{Y_{\delta q}}\cos\beta - C_{N_{\delta q}}\sin\alpha\sin\beta)\delta q$$
$$-(C_{Y_{\delta r}}\cos\beta - C_{N_{\delta r}}\sin\alpha\sin\beta)\delta r] \quad (3)$$

$$\dot{\mu} = p\frac{\cos\alpha}{\cos\beta} + r\frac{\sin\alpha}{\cos\beta} + \frac{T}{MV}[\sin\alpha\sin\mu\tan\gamma - \cos\alpha\sin\beta\cos\mu\tan\gamma$$
$$+\sin\alpha\tan\beta] + \frac{\bar{q}S}{MV}[-C_A\sin\alpha(\sin\mu\tan\gamma + \tan\beta)$$
$$+C_A\cos\alpha\cos\mu\sin\beta\tan\gamma + C_{N_0}\cos\alpha(\sin\mu\tan\gamma + \tan\beta)$$
$$+C_{N_0}\sin\alpha\cos\mu\sin\beta\tan\gamma + C_{Y_0}\cos\mu\cos\beta\tan\gamma]$$
$$-\frac{g}{V}\cos\gamma\cos\mu\tan\beta + \frac{\bar{q}S}{MV}[C_{N_{\delta p}}\delta p - C_{N_{\delta q}}\delta q$$
$$-C_{N_{\delta r}}\delta r][\cos\alpha(\sin\mu\tan\gamma + \tan\beta) + \sin\alpha\cos\mu\sin\beta\tan\gamma]$$
$$+\frac{\bar{q}S}{MV}[C_{Y_{\delta p}}\delta p - C_{Y_{\delta q}}\delta q - C_{Y_{\delta r}}\delta r]\cos\mu\cos\beta\tan\gamma \quad (4)$$

$$\dot{p} = \frac{I_y - I_z}{I_x}qr + \frac{\bar{q}Sd^2}{2I_xV}(C_{l_p}\cos\alpha p - C_{n_r}\sin\alpha r) + \frac{\bar{q}Sd}{I_x}(C_{l_0}\cos\alpha$$
$$-C_{n_0}\sin\alpha) + \frac{\bar{q}Sd}{I_x}[(C_{l_{\delta p}}\cos\alpha - C_{n_{\delta p}}\sin\alpha)\delta p - (C_{l_{\delta q}}\cos\alpha$$
$$-C_{n_{\delta q}}\sin\alpha)\delta q - (C_{l_{\delta r}}\cos\alpha - C_{n_{\delta r}}\sin\alpha)\delta r] \quad (5)$$

$$\dot{q} = \frac{I_z - I_x}{I_y}rp + \frac{\bar{q}Sd^2}{2I_yV}C_{m_q}q + \frac{\bar{q}Sd}{I_y}(C_{m_0} + C_{m_{\delta p}}\delta p - C_{m_{\delta q}}\delta q - C_{m_{\delta r}}\delta r) \quad (6)$$

$$\dot{r} = \frac{I_x - I_y}{I_z}pq + \frac{\bar{q}Sd^2}{2I_zV}(C_{l_p}\sin\alpha p + C_{n_r}\cos\alpha r) + \frac{\bar{q}Sd}{I_z}(C_{l_0}\sin\alpha$$
$$+C_{n_0}\cos\alpha) + \frac{\bar{q}Sd}{I_z}[(C_{l_{\delta p}}\sin\alpha + C_{n_{\delta p}}\cos\alpha)\delta p - (C_{l_{\delta q}}\sin\alpha$$
$$+C_{n_{\delta q}}\cos\alpha)\delta q - (C_{l_{\delta r}}\sin\alpha + C_{n_{\delta r}}\cos\alpha)\delta r] \quad (7)$$

2

3. The SDRE Method

Consider the autonomous, infinite-horizon, non-linear regulator problem for minimizing the performance index

$$J = \frac{1}{2} \int_0^\infty x^T Q(x) x + u^T R(x) u \ dt \qquad (8)$$

with respect to the state x and control u subject to the nonlinear differential constraints:

$$\dot{x} = f(x) + B(x)u \qquad (9)$$

where $Q(x) \geq 0$ and $R(x) > 0$ for all x and $f(0) = 0$.

The SDRE approach for obtaining a suboptimal, locally asymptotically stabilizing solution of problem (8)-(9) is:

i) *Use direct parameterization to bring the nonlinear dynamics to the state-dependent coefficient (SDC) form*

$$\dot{x} = A(x)x + B(x)u \qquad (10)$$

where

$$f(x) = A(x)x \qquad (11)$$

In the multivariable case, it is well-known [16] that if $f(x)$ is a continuously differentiable function of x, there is an infinite number of ways to factor $f(x)$ into $A(x)x$. In order to obtain a valid solution of the SDRE, the pair $\{A(x), B(x)\}$ has to be pointwise stabilizable in the linear sense for all x in the domain of interest.

ii) *Solve the state-dependent Riccati equation*

$$A^T P + PA - PBR^{-1}B^T P + Q = 0 \qquad (12)$$

to obtain $P(x) \geq 0$.

iii) *Construct the nonlinear feedback controller equation:*

$$u = -R(x)^{-1} B(x)^T P(x) x. \qquad (13)$$

In order to perform command following, the SDRE controller can be implemented as an integral servo-mechanism as demonstrated in [17]. This is accomplished as follows. First, the state x is decomposed as

$$x = \begin{bmatrix} x_T \\ x_N \end{bmatrix} \qquad (14)$$

where it is desired for the vector components of x_T to track a reference command r_c. The state vector x is then augmented with x_I, the integral states of x_T:

$$\tilde{x} = \begin{bmatrix} x_I \\ x_T \\ x_N \end{bmatrix} \qquad (15)$$

The augmented system is given by

$$\dot{\tilde{x}} = \tilde{A}(\tilde{x})\tilde{x} + \tilde{B}(\tilde{x})u \qquad (16)$$

where

$$\tilde{A}(\tilde{x}) = \begin{bmatrix} 0 & I \\ A(x) & 0 \end{bmatrix} \quad \tilde{B}(\tilde{x}) = \begin{bmatrix} 0 \\ B(x) \end{bmatrix} \qquad (17)$$

and the SDRE integral servo controller is given by

$$u = -\tilde{R}(\tilde{x})^{-1} \tilde{B}(\tilde{x})^T \tilde{P}(\tilde{x}) \begin{bmatrix} x_I - \int r_c dt \\ x_T - r_c \\ x_N \end{bmatrix} \qquad (18)$$

In order for the SDRE to have a solution, the pointwise detectability condition must be satisfied. This is accomplished by penalizing the integral states with the corresponding non-zero diagonal elements of $\tilde{Q}(\tilde{x})$.

4. SDRE Control Design

The autopilot has the two-loop structure shown in Figure 1. Guidance law acceleration commands are converted into angle-of-attack, sideslip, and bank-angle commands, α_c, β_c, μ_c, using the BTT/STT Logic presented in Section 5. The outer loop converts α_c, β_c, μ_c to roll-rate, pitch-rate, and yaw-rate commands, p_c, q_c, r_c, for the inner loop. The inner loop then converts p_c, q_c, r_c to fin commands for the actuators.
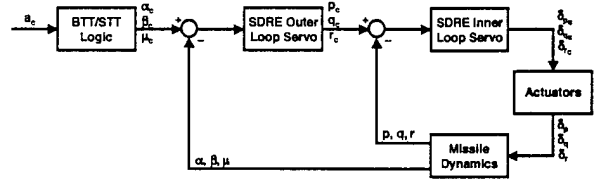

Figure 1: Autopilot Two-Loop Structure

3

SDRE Outer-Loop Integral Servomechanism

For the outer loop, the state space is given by

$$\tilde{x} = \begin{bmatrix} V & \alpha_I & \alpha & \beta_I & \beta & \mu_I & \mu \end{bmatrix}^T$$

$$u = \begin{bmatrix} p & q & r \end{bmatrix}^T \qquad (19)$$

The current values of the fins $\delta p, \delta q, \delta r$ are used in this loop which is based on Eqs. (1)-(4). The state-dependent factorization $\{\tilde{A}(\tilde{x}), \tilde{B}(\tilde{x})\}$ for the outer loop controller is given in the Appendix. Since thrust is not controllable, the controllability of the speed equation is due to α and β. Speed controllability is lost when α and β are both zero and ill-conditioning occurs in the Riccati equation when α and β are small. A stablizing term of $-10V$ was added to the speed equation in the controller to eliminate the ill-conditioning.

SDRE Inner-Loop Servomechanism

For the inner loop, a hard bound of 30 degrees was imposed on the controls (the fin commands) and an SDRE servo was used instead of an integral servo. The hard bound is achieved by replacing $\delta p, \delta q, \delta r$ in Eqs. (5)-(7) with saturation sine functions and using integral control. The saturation sine function (satsin) is defined as

$$\text{satsin}(m, z) = \begin{cases} m * \sin(z) & \text{for} & |z| < \frac{\pi}{2}, \\ m & \text{for} & z \geq \frac{\pi}{2}, \\ -m & \text{for} & z \leq -\frac{\pi}{2} \end{cases} \qquad (20)$$

and is plotted in Figure 2 for $m = 1$.

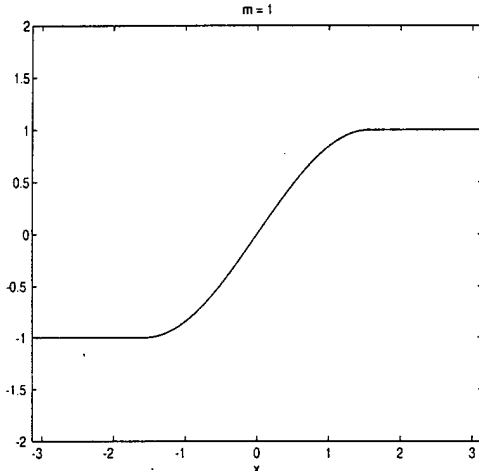Figure 2: Saturation Sine Function

We have

$$\begin{bmatrix} \delta p \\ \delta q \\ \delta r \end{bmatrix} = \begin{bmatrix} \text{satsin}(30, \widetilde{\delta p}) \\ \text{satsin}(30, \widetilde{\delta q}) \\ \text{satsin}(30, \widetilde{\delta r}) \end{bmatrix} \qquad (21)$$

with the fin coefficients expressed in units of per degree and

$$\dot{\widetilde{\delta p}} = -\lambda_p(\widetilde{\delta p} - u_p) \qquad (22)$$

$$\dot{\widetilde{\delta q}} = -\lambda_q(\widetilde{\delta q} - u_q) \qquad (23)$$

$$\dot{\widetilde{\delta r}} = -\lambda_r(\widetilde{\delta r} - u_r) \qquad (24)$$

with $\lambda_p, \lambda_q, \lambda_r$ being design parameters and u_p, u_q, u_r being the new controls. Note that in Eqs. (5)-(7), the terms $\bar{q}Sd(C_{l_0}\cos\alpha - C_{n_0}\sin\alpha)/I_x$, $\bar{q}SdC_{m_0}/I_y$, and $\bar{q}Sd(C_{l_0}\sin\alpha + C_{n_0}\cos\alpha)/I_z$ are bias terms, i.e., state-independent terms. Normally, bias terms can be handled within the SDRE framework by multiplying and dividing these terms by a state that will never go to zero. Since p, q, r and $\delta p, \delta q, \delta r$ can all go to zero, an additional state s with stable dynamics was added to the control equations for the purpose of absorbing the biases:

$$\dot{s} = -\lambda_s s \qquad (25)$$

At each pass through the inner loop, s is set to its initial value. Thus, for the inner loop, the state space is given by

$$\tilde{x} = \begin{bmatrix} p & q & r & s & \widetilde{\delta p} & \widetilde{\delta q} & \widetilde{\delta r} \end{bmatrix}^T$$

$$u = \begin{bmatrix} u_p & u_q & u_r \end{bmatrix}^T \qquad (26)$$

with the fin commands being computed from Eq. (21). The state-dependent factorization $\{\tilde{A}(\tilde{x}), \tilde{B}(\tilde{x})\}$ for the inner loop controller is given in the Appendix.

Measurement and Estimation of the States

If measurements of α and β are not available, there are at least two means of producing estimates of these variables. One is to use a nonlinear observer that is based on Eqs. (2) and (3) augmented with the forcing terms $K_\alpha[a_z - \bar{q}SC_Z(\hat{\alpha}, \mathcal{M})/M]$ and $K_\beta[a_y - \bar{q}SC_Y(\hat{\beta}, \mathcal{M})/M]$, respectively, where K_α and K_β are the observer gains. The observer adjusts the estimates of α and β based on the difference between the measured and predicted body accelerations. A second way is design a filter based on Eqs. (2), (3), (5), and (7) whose measurements are the body rates p, q, and r. With α and β estimated, the bank angle μ can be computed as

$$\mu = \tan^{-1}\left(\frac{\sin\theta\cos\hat{\alpha}\sin\hat{\beta} - \cos\theta(\cos\phi\sin\hat{\alpha}\sin\hat{\beta} - \sin\phi\cos\hat{\beta})}{\cos\phi\cos\theta\cos\hat{\alpha} + \sin\theta\sin\hat{\alpha}}\right)$$

The body accelerations and the body rates can be measured from the strapdown inertial measurement unit (IMU).

5. Bank-to-Turn/Skid-to-Turn Command Logic

BTT control is used in the midcourse and terminal phases of flight to prevent the air-breathing engine from flaming out. The BTT mode is broken into three commanded-acceleration magnitude regions in the inertial-frame (I) as defined below:

If $a_c^I < .1g$ then STT Control
$$\mu_c = \mu$$

If $.1g \leq a_c^I < 1g$ then Reduced BTT Control
$$\mu_c = \mu + \left[\tan^{-1}\left(\frac{-a_{y_c}^I}{a_{z_c}^I}\right) - \mu\right]\frac{a_c^I}{1g}$$

If $a_c^I \geq 1g$ then Full BTT Control
$$\mu_c = \tan^{-1}\left(\frac{-a_{y_c}^I}{a_{z_c}^I}\right)$$

In full BTT mode,
$$\alpha_c = \frac{(\|a_c\|M/\bar{q}S) - |(C_Z - C_{Z_\alpha}\alpha)|}{|C_{Z_\alpha}|}$$
$$\beta_c = 0$$

where $a_c = [a_{y_c}\ a_{z_c}]^T$ is the commanded acceleration in the body frame.

In reduced BTT mode,
$$\alpha_c = \frac{(\|a_c\|M/\bar{q}S) - |(C_Z - C_{Z_\alpha}\alpha)|}{|C_{Z_\alpha}|}\cos(\mu_{full} - \mu_c)$$
$$\beta_c = \frac{(\|a_c\|M/\bar{q}S) - (C_Y - C_{Y_\beta}\beta)}{C_{Y_\beta}}\sin(\mu_{full} - \mu_c)$$

where
$$\mu_{full} = \tan^{-1}\left(\frac{-a_{y_c}^I}{a_{z_c}^I}\right).$$

Note that STT is used for small acceleration commands to prevent the missile from performing 180° rolls to achieve insignificant accelerations. STT control is also used in the endgame for quicker response.

In the STT mode,
$$\alpha_c = \frac{(a_{z_c}M/\bar{q}S) - (C_Z - C_{Z_\alpha}\alpha)}{C_{Z_\alpha}}$$
$$\beta_c = \frac{(a_{y_c}M/\bar{q}S) - (C_Y - C_{Y_\beta}\beta)}{C_{Y_\beta}}$$
$$\mu_c = \mu$$

As the missile approaches the endgame phase and passes a preset time-to-go threshold, STT commands are ramped into the BTT commands over a preselected time interval to attenuate transient responses, i.e.,

$$\begin{bmatrix}\alpha_c \\ \beta_c \\ \mu_c\end{bmatrix} = \rho\begin{bmatrix}\alpha_c \\ \beta_c \\ \mu_c\end{bmatrix}_{STT} + (1-\rho)\begin{bmatrix}\alpha_c \\ \beta_c \\ \mu_c\end{bmatrix}_{BTT}$$

where ρ is a parameter that varies linearly from zero to one over the specified time interval.

6. Simulation Results

An investigation of the performance of the autopilot has been conducted using a detailed six-degrees-of-freedom simulation. The simulation imposes rate limits of 500°/sec on p and 200°/sec on q and r. The fin deflection limit is 30° and the actuator dynamics have a time constant of .01. In order to maintain good autopilot response over the flight envelope, the state weighting on $\alpha_I, \alpha, \beta_I, \beta$ was varied at low, medium and high altitudes until similar performance was achieved. The state weights were then curve fit to a quadratic function of dynamic pressure, $\bar{q}$, which in turn is a function of missile velocity, one of the states in the outer-loop (OL). The following state and control weighting matrices were selected for the outer-loop controller:

$$\bar{Q}(\tilde{x})_{OL} = \begin{bmatrix} 0 & 0 & 0 & 0 & 0 & 0 & 0 \\ 0 & q_{22}(\tilde{x}) & 0 & 0 & 0 & 0 & 0 \\ 0 & 0 & q_{33}(\tilde{x}) & 0 & 0 & 0 & 0 \\ 0 & 0 & 0 & q_{44}(\tilde{x}) & 0 & 0 & 0 \\ 0 & 0 & 0 & 0 & q_{55}(\tilde{x}) & 0 & 0 \\ 0 & 0 & 0 & 0 & 0 & q_{66}(\tilde{x}) & 0 \\ 0 & 0 & 0 & 0 & 0 & 0 & 100 \end{bmatrix}$$

$$\bar{R}(\tilde{x})_{OL} = \begin{bmatrix} 1 & 0 & 0 \\ 0 & 1 & 0 \\ 0 & 0 & 1 \end{bmatrix}$$

where

$$q_{22}(\tilde{x}) = 9.7285 * 10^{-11}\bar{q}(\tilde{x})^2 + 1.6818 * 10^{-5}\bar{q}(\tilde{x}) + .5114$$

$$q_{33}(\tilde{x}) = 9.5209 * 10^{-10}\bar{q}(\tilde{x})^2 - 1.7642 * 10^{-4}\bar{q}(\tilde{x}) + 88.1654$$

$$q_{44}(\tilde{x}) = q_{22}(\tilde{x})$$

$$q_{55}(\tilde{x}) = q_{33}(\tilde{x})$$

$$q_{66}(\tilde{x}) = \min\{100, [(\mu - \mu_c)180/\pi]^2 + .001\}$$

5

By using a state-dependent weighting on the integral of μ, we were able to enhance the rise time and reduce the overshoot of the μ response. At the same time, the state weighting on q and r was also varied at low, medium and high altitudes to aid in achieving the desired performance. Similarly, the state weights were curve fit to a quadratic function of dynamic pressure, $\bar{q}$, which is a parameter that is provided to the inner-loop (IL) controller. The inner-loop state and control weightings were chosen to be:

$$\bar{Q}(\tilde{x})_{IL} = \begin{bmatrix} 20 & 0 & 0 & 0 & 0 & 0 & 0 \\ 0 & q_{22} & 0 & 0 & 0 & 0 & 0 \\ 0 & 0 & q_{33} & 0 & 0 & 0 & 0 \\ 0 & 0 & 0 & 0 & 0 & 0 & 0 \\ 0 & 0 & 0 & 0 & 0 & 0 & 0 \\ 0 & 0 & 0 & 0 & 0 & 0 & 0 \\ 0 & 0 & 0 & 0 & 0 & 0 & 0 \end{bmatrix}$$

$$\bar{R}(\tilde{x})_{IL} = \begin{bmatrix} .01 & 0 & 0 \\ 0 & .01 & 0 \\ 0 & 0 & .01 \end{bmatrix}$$

where

$$q_{22} = 1.7187 * 10^{-10}\bar{q}^2 - 1.9783 * 10^{-4}\bar{q} + 57.3033$$
$$q_{33} = 1.6329 * 10^{-10}\bar{q}^2 - 1.9498 * 10^{-4}\bar{q} + 117.1089$$

The inverse time constants used were $\lambda_p = \lambda_q = \lambda_r = \lambda_s = 1$.

The autopilot was evaluated at three different flight conditions, the first being the initial design condition of $\mathcal{M} = 2.7$, $h = 20000\ ft$. The second and third flight conditions were at the missiles minimum altitude $\mathcal{M} = 2.7$, $h = 100\ ft$ and at a high altitude $\mathcal{M} = 2.7$, $h = 40000\ ft$, respectively. A commanded inertial acceleration of $a_{y_c} = 10g$, $a_{z_c} = -10g$ was rotated into the body frame and used as input into the BTT/STT command logic and the vehicle responded in the BTT mode. Figures 3-10 illustrate the performance of the autopilot at flight condition one and Figures 11-18 illustrate the performance of the autopilot at all three flight conditions (0.1 Kft - Dark, 20 Kft - Medium, 40 Kft - Light). Figures 3-5 and 11-13 show the outer-loop tracking of α_c, β_c, μ_c and Figures 6-8 and 14-16 show the inner-loop tracking of p_c, q_c, r_c. Figures 9 and 17 show the fin deflections for the two cases. Figures 10 and 18 show the autopilot tracking of the acceleration commands coming from the guidance law. As can be seen, both the inner and outer loop controllers are well-behaved and provide excellent tracking and response over a large region of the operating envelope. Further analysis of the operating envelope may result in additional scheduling of the weights in the inner and outer loop controllers as a function of dynamic pressure.
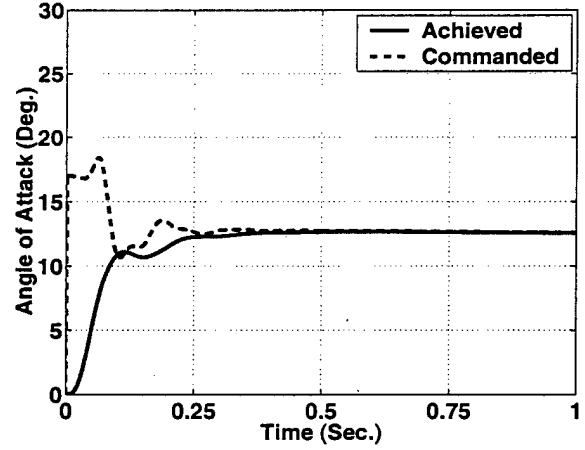

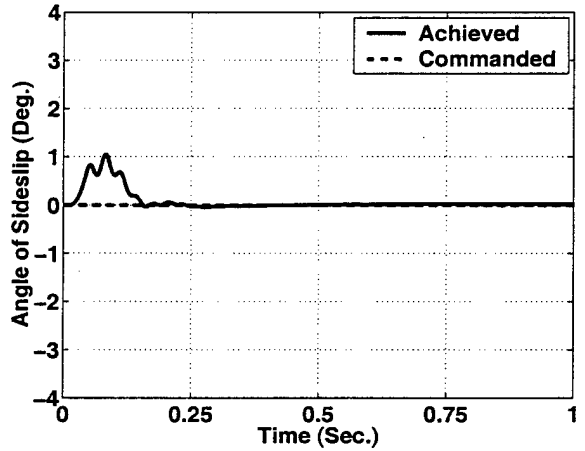Figure 3: Commanded and Achieved Angles of Attack ($\mathcal{M} = 2.7, h = 20Kft$)

Figure 4: Commanded and Achieved Angles of Sideslip ($\mathcal{M} = 2.7, h = 20Kft$)
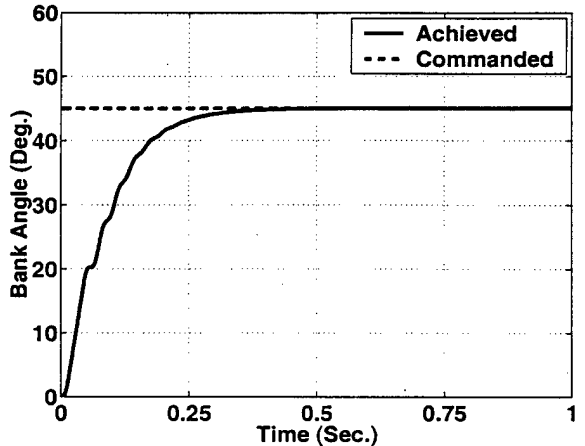

Figure 5: Commanded and Achieved Bank Angles ($\mathcal{M} = 2.7, h = 20Kft$)

Figure 6: Commanded and Achieved Roll Rates ($\mathcal{M} = 2.7, h = 20Kft$)

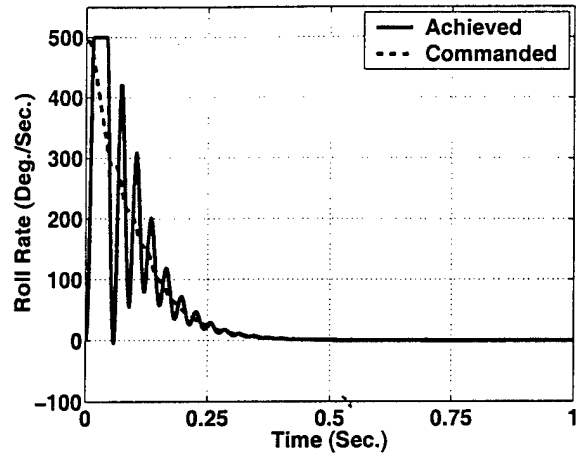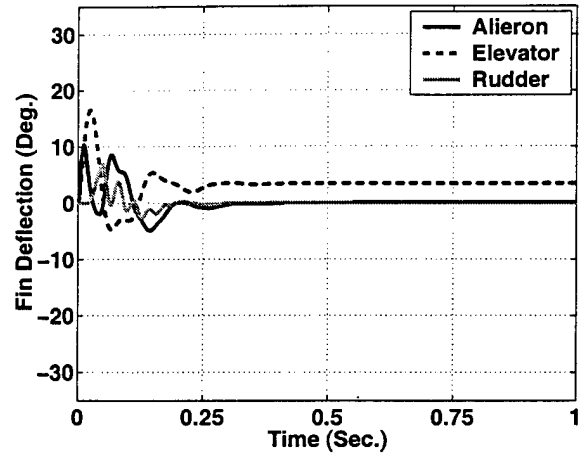Figure 7: Commanded and Achieved Pitch Rates ($\mathcal{M} = 2.7, h = 20Kft$)

Figure 8: Commanded and Achieved Yaw Rates ($\mathcal{M} = 2.7, h = 20Kft$)

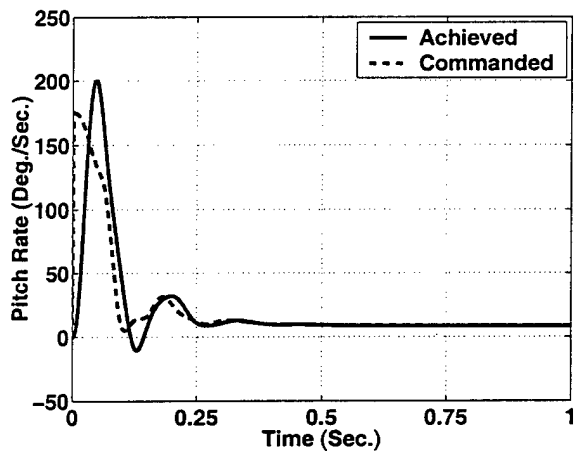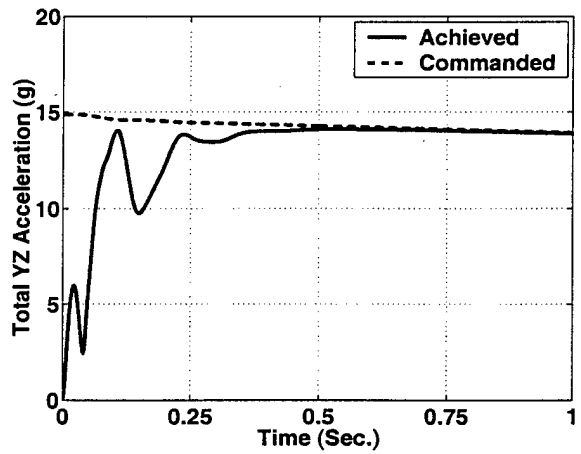Figure 9: Achieved Fin Deflections ($\mathcal{M} = 2.7, h = 20Kft$)

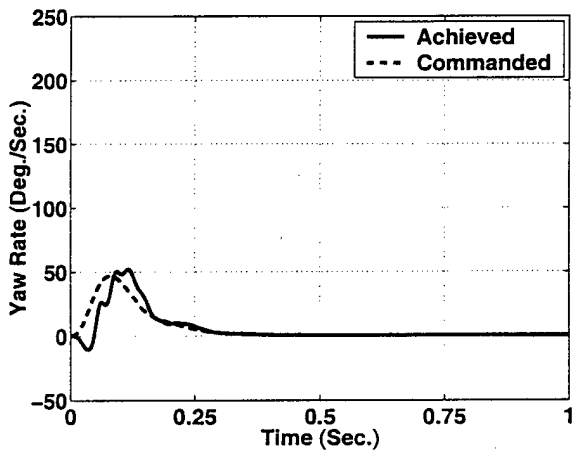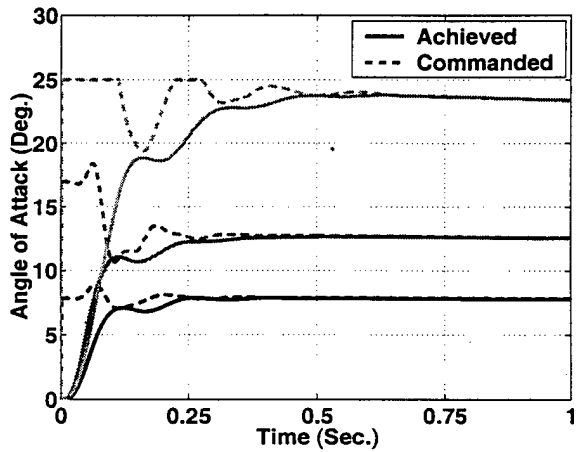Figure 10: Commanded and Achieved Body Accelerations ($\mathcal{M} = 2.7, h = 20Kft$)

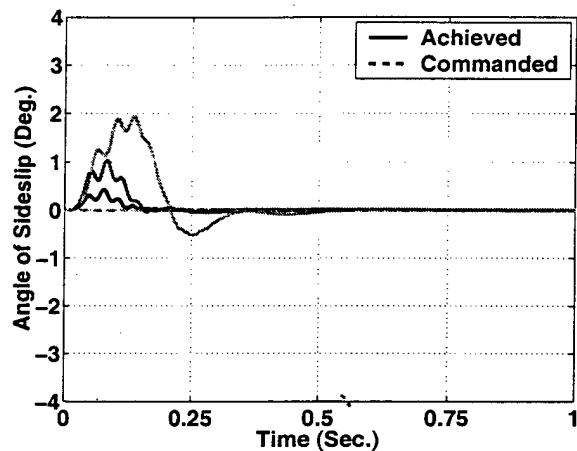Figure 11: Commanded and Achieved Angles of Attack ($\mathcal{M} = 2.7, h = 0.1, 20, 40Kft$)

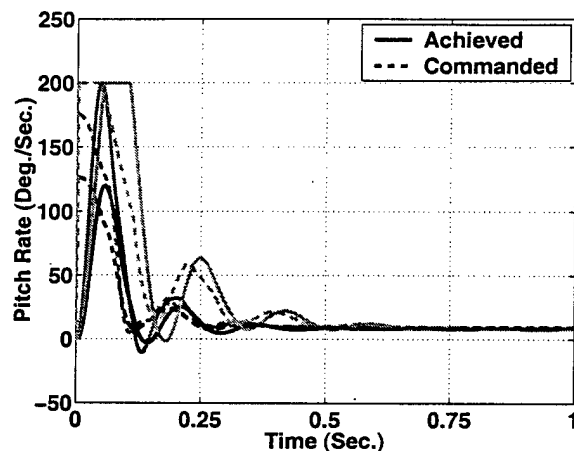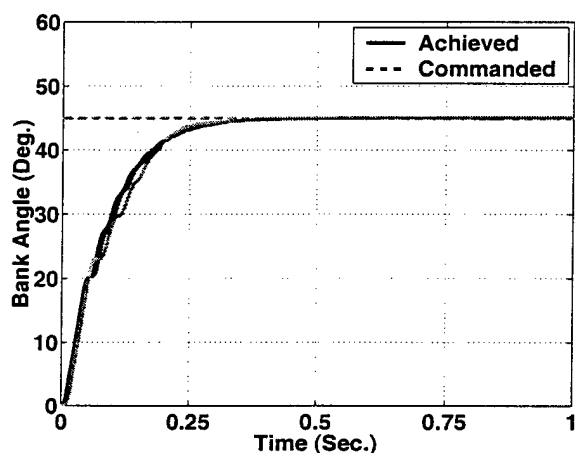Figure 12: Commanded and Achieved Angles of Sideslip ($\mathcal{M} = 2.7, h = 0.1, 20, 40Kft$)

Figure 13: Commanded and Achieved Bank Angles ($\mathcal{M} = 2.7, h = 0.1, 20, 40Kft$)

Figure 14: Commanded and Achieved Roll Rates ($\mathcal{M} = 2.7, h = 0.1, 20, 40Kft$)

Figure 15: Commanded and Achieved Pitch Rates ($\mathcal{M} = 2.7, h = 0.1, 20, 40Kft$)

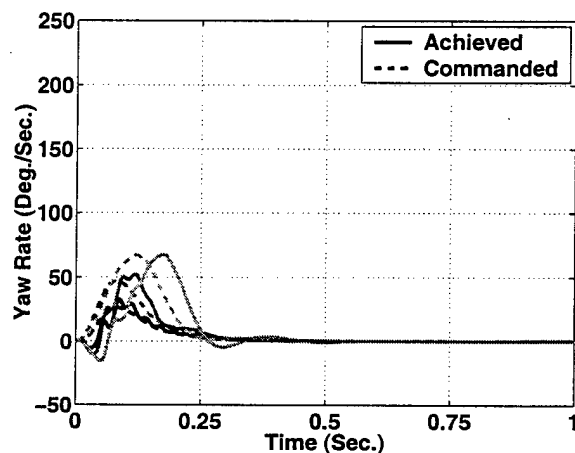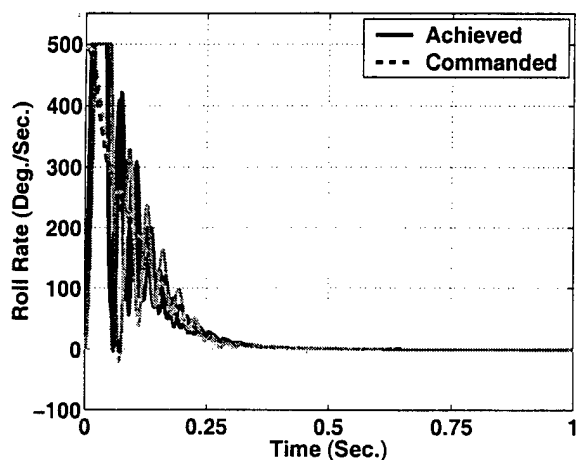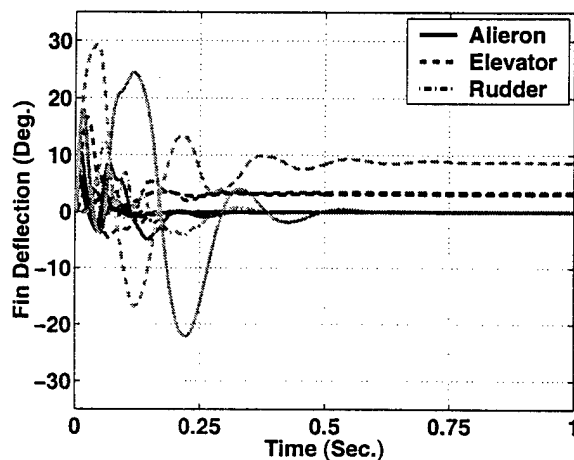Figure 16: Commanded and Achieved Yaw Rates ($\mathcal{M} = 2.7, h = 0.1, 20, 40Kft$)

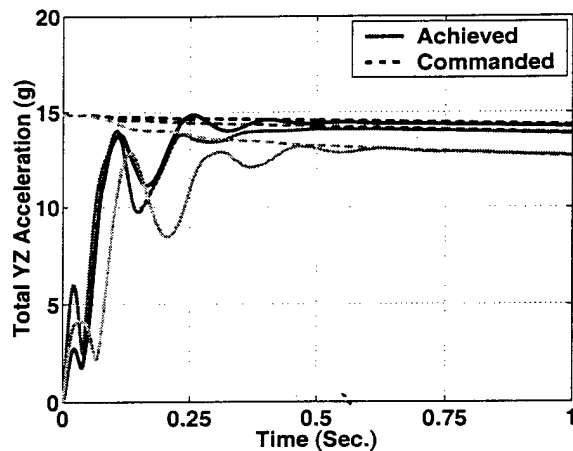Figure 17: Achieved Fin Deflections ($\mathcal{M} = 2.7, h = 0.1, 20, 40Kft$)

Figure 18: Commanded and Achieved Body Accelerations ($\mathcal{M} = 2.7, h = 0.1, 20, 40Kft$)

7. Summary

The SDRE control method has been used to design a hybrid bank-to-turn/skid-to-turn autopilot for a generic air-breathing air-to-air missile. The autopilot is broken into an outer loop and an inner loop. The outer loop converts commanded angle-of-attack, sideslip, and bank angle to body rate commands for the inner loop. The inner loop converts the body rate commands to fin deflection commands. Hard bounds on the fin deflections are embedded within the inner-loop controller dynamics so the autopilot only commands fin deflections that are achievable. The design results are very promising and it is expected that the autopilot will provide excellent performance in an air-to-air intercept scenario. Future work will include flying air-to-air intercepts to exercise the BTT, hybrid BTT/STT, and STT modes of the controller. Additionally, a wind model will be incorporated into the simulation to validate the α and β observers. Finally, the robustness of the autopilot will be evaluated in the presence of uncertainties in the aerodynamic coefficients.

References

[1] Bossi, J. A., Langehough, M. A., *Multivariable Autopilot Design for a Bank-to-Turn Missile*, Proceedings of the American Controls Conference, Atlanta, GA, June, 1988.

[2] Nichols, R. A., Reichert, R. T., and Rugh, W. J., *Gain Scheduling for H-Infinity Controllers: A Flight Control Example*, IEEE Transactions on Control System Technology, Vol 1, No. 2, 1993, pp. 69-79.

[3] Blakelock, J. H., *Automatic Control of Aircraft and Missiles*, John Wiley & Sons, Inc., New York, 1991.

[4] Shamma, J. S. and Athans, M., *Analysis of Gain Scheduled Control for Nonlinear Plants*, IEEE Transactions on Automatic Control, Vol 35, No. 8, 1990, pp. 898-907.

[5] Kaloust J. K., Schroeder, W., and Cable, C., *Stall and Recovery Control System (SARCS): A Nonlinear Autopilot Controller for Airborne Vehicles*, Proceedings of the AIAA Guidance, Navigation and Control Conference, Denver, CO, August, 2000.

[6] McFarland M. B. and Hoque, S. M., *Robustness of a Nonlinear Missile Autopilot Designed Using Dynamic Inversion*, Proceedings of the AIAA Guidance, Navigation and Control Conference, Denver, CO, August, 2000.

[7] Mickle, M. C., Zhu, J. J., *Bank-To-Turn Roll-Yaw-Pitch Autopilot Design Using Dynamic Nonlinear Inversion and PD-Eigenvalue Assignment*, Proceedings of the American Controls Conference, Chicago, IL, June, 2000.

[8] Shkolnikov, I. A., Shtessel, Y. B., Lianos, D., and Thies, A. T., *Robust Missile Autopilot Design Via High-Order Sliding Mode Control*, Proceedings of the AIAA Guidance, Navigation and Control Conference, Denver, CO, August, 2000.

[9] McDowell, D. M., Irwin, G. W., and McConnell, G., *Online Neural Control Applied to a Bank-to-Turn Missile Autopilot*, Proceedings of the AIAA Guidance, Navigation and Control Conference, Baltimore, MD, August, 1995.

[10] Wu, F., Packard, A. K., and Balas, G. J., *LPV Control Design for Pitch-Axis Missile Autopilots*, Proceedings of the IEEE Conference on Decision and Control, New Orleans, LA, December, 1995.

[11] Tan, W., Packard, A. K., and Balas, G. J., *Quasi-LPV Modeling and LPV Control of Generic Missile*, Proceedings of the American Controls Conference, Chicago, IL, June, 2000.

[12] Mracek, C. P. and Cloutier, J. R. *Full Envelope Missile Longitudinal Autopilot Design Using the State-Dependent Riccati Equation Method*, Proceedings of the AIAA Guidance, Navigation and Control Conference, New Orleans, LA, August, 1997.

[13] Menon, P. K. and Iragavarapu, V. R., *Integrated Design of Agile Missile Guidance and Control Systems*, Naval Surface Warfare Center SBIR Report, Dahlgren, VA, October 1997.

[14] Palumbo, N. F.and Jackson, T. D., *Development of a Fully Integrated Missile Guidance and Control System: A State Dependent Riccati Differential Equation Approach*, Proceedings of the IEEE Conference on Control Applications Hawaii, HI, August, 1999.

[15] Dahlene, L. P., *Aerodynamic Database and Model Development for Munitions*, AFRL/MN High School Apprentice Program Report, Eglin AFB, FL, August 2000.

[16] Cloutier, J. R., Mracek, C. P., Ridgely, D. B., and Hammett, K. D., *State-Dependent Riccati Equation Techniques: Theory and Applications*, Notes from the SDRE Workshop Conducted at the American Control Conference, Philadelphia, PA, June 1998.

[17] Cloutier, J. R. and Stansbery, D. T., *Control of a Continuously Stirred Tank Reactor Using an Asymmetric Solution of the State-Dependent Riccati Equation*, Proceedings of the IEEE Conference on Control Applications Hawaii, HI, August, 1999.

Appendix

Outer-Loop State-Dependent Coefficient Factorization

$$\bar{A}(\bar{x}) = \begin{bmatrix} a11 & 0 & a13 & 0 & a15 & 0 & 0 \\ 0 & 0 & 1 & 0 & 0 & 0 & 0 \\ a31 & 0 & a33 & 0 & 0 & 0 & 0 \\ 0 & 0 & 0 & 0 & 1 & 0 & 0 \\ a51 & 0 & a53 & 0 & a55 & 0 & a57 \\ 0 & 0 & 0 & 0 & 0 & 0 & 1 \\ a71 & 0 & a73 & 0 & a75 & 0 & a77 \end{bmatrix}$$

where

$$a11 = -10 - \frac{\bar{q}S}{MV}C_A \cos\alpha \cos\beta - \frac{g}{V}\sin\gamma + \frac{T}{MV}\cos\alpha \cos\beta$$
$$+ \frac{\bar{q}S}{MV}(C_{Y_{\delta p}}\sin\beta - C_{N_{\delta p}}\sin\alpha \cos\beta)\delta p$$
$$- \frac{\bar{q}S}{MV}(C_{Y_{\delta q}}\sin\beta - C_{N_{\delta q}}\sin\alpha \cos\beta)\delta q$$
$$- \frac{\bar{q}S}{MV}(C_{Y_{\delta r}}\sin\beta - C_{N_{\delta r}}\sin\alpha \cos\beta)\delta r$$

$$a13 = -\frac{\bar{q}S}{M}C_{N_0}\frac{\sin\alpha}{\alpha}\cos\beta$$

$$a15 = \frac{\bar{q}S}{M}C_{Y_0}\frac{\sin\beta}{\beta}$$

$$a31 = \frac{g}{V^2\cos\beta}\cos\gamma \cos\mu - \frac{\bar{q}S}{MV^2\cos\beta}\cos\alpha C_{N_0}$$
$$- \frac{\bar{q}S}{MV^2\cos\beta}\cos\alpha(C_{N_{\delta p}}\delta p - C_{N_{\delta q}}\delta q - C_{N_{\delta r}}\delta r)$$

$$a33 = -\frac{T}{MV\cos\beta}\frac{\sin\alpha}{\alpha} + \frac{\bar{q}S}{MV\cos\beta}C_A\frac{\sin\alpha}{\alpha}$$

$$a51 = \frac{\bar{q}S}{MV^2}C_{Y_0}\cos\beta + (C_{Y_{\delta p}}\cos\beta + C_{N_{\delta p}}\sin\alpha \sin\beta)\delta p$$
$$- (C_{Y_{\delta q}}\cos\beta + C_{N_{\delta q}}\sin\alpha \sin\beta)\delta q$$
$$- (C_{Y_{\delta r}}\cos\beta + C_{N_{\delta r}}\sin\alpha \sin\beta)\delta r$$

$$a53 = \alpha_1 \frac{\bar{q}S}{MV}C_{N_0}\frac{\sin\alpha}{\alpha}\sin\beta$$

$$a55 = (1 - \alpha_1)\frac{\bar{q}S}{MV}C_{N_0}\sin\alpha\frac{\sin\beta}{\beta} + \left(\frac{\bar{q}S}{MV}C_A - \frac{T}{MV}\right)\cos\alpha\frac{\sin\beta}{\beta}$$

$$a57 = \frac{g}{V}\cos\gamma\frac{\sin\mu}{\mu}$$

$$a71 = \frac{\bar{q}S}{MV^2}(C_{Y_0} + C_{Y_{\delta p}}\delta p - C_{Y_{\delta q}}\delta q - C_{Y_{\delta r}}\delta r)\cos\mu \cos\beta \tan\gamma$$

$$a73 = \alpha_2 \frac{T}{MV}\frac{\sin\alpha}{\alpha}\sin\mu \tan\gamma + \alpha_3 \frac{T}{MV}\frac{\sin\alpha}{\alpha}\tan\beta$$
$$- \alpha_4 \frac{\bar{q}S}{MV}C_A\frac{\sin\alpha}{\alpha}\sin\mu \tan\gamma - \alpha_5 \frac{\bar{q}S}{MV}C_A\frac{\sin\alpha}{\alpha}\tan\beta$$
$$+ \alpha_6 \frac{\bar{q}S}{MV}(C_{N_0} + C_{N_{\delta p}}\delta p - C_{N_{\delta q}}\delta q - C_{N_{\delta r}}\delta r)\frac{\sin\alpha}{\alpha}\cos\mu \sin\beta \tan\gamma$$

$$a75 = -\frac{T}{MV}\cos\alpha\frac{\sin\beta}{\beta}\cos\mu \tan\gamma$$
$$+ (1 - \alpha_3)\frac{T}{MV}\cos\beta \sin\alpha\frac{\sin\beta}{\beta}$$
$$- (1 - \alpha_5)\frac{\bar{q}S}{MV\cos\beta}C_A \sin\alpha\frac{\sin\beta}{\beta}$$
$$+ \frac{\bar{q}S}{MV\cos\beta}(C_{N_0} + C_{N_{\delta p}}\delta p - C_{N_{\delta q}}\delta q - C_{N_{\delta r}}\delta r)\cos\alpha\frac{\sin\beta}{\beta}$$
$$+ \frac{\bar{q}S}{MV}C_A \cos\alpha \cos\mu\frac{\sin\beta}{\beta}\tan\gamma$$
$$+ (1 - \alpha_6)\frac{\bar{q}S}{MV}(C_{N_0} + C_{N_{\delta p}}\delta p - C_{N_{\delta q}}\delta q$$
$$- C_{N_{\delta r}}\delta r)\sin\alpha \cos\mu\frac{\sin\beta}{\beta}\tan\gamma - \frac{g}{V\cos\beta}\cos\gamma \cos\mu\frac{\sin\beta}{\beta}$$

$$a77 = (1 - \alpha_2)\frac{T}{MV}\sin\alpha\frac{\sin\mu}{\mu}\tan\gamma$$
$$- (1 - \alpha_4)\frac{\bar{q}S}{MV}C_A \sin\alpha\frac{\sin\mu}{\mu}\tan\gamma$$
$$+ \frac{\bar{q}S}{MV}(C_{N_0} + C_{N_{\delta p}}\delta p - C_{N_{\delta q}}\delta q - C_{N_{\delta r}}\delta r)\cos\alpha\frac{\sin\mu}{\mu}\tan\gamma$$

Presently, the α_i's have been selected as

$$\alpha_1 = \alpha_2 = \alpha_3 = \alpha_4 = \alpha_5 = \alpha_6 = .5$$

$$\bar{B}(\bar{x}) = \begin{bmatrix} 0 & 0 & 0 \\ 0 & 0 & 0 \\ -\tan\beta \cos\alpha & 1 & -\tan\beta \sin\alpha \\ 0 & 0 & 0 \\ \sin\alpha & 0 & -\cos\alpha \\ 0 & 0 & 0 \\ \frac{\cos\alpha}{\cos\beta} & 0 & \frac{\sin\alpha}{\cos\beta} \end{bmatrix}$$

Inner-Loop State-Dependent Coefficient Factorization

$$\tilde{A}(\tilde{x}) = \begin{bmatrix} a11 & a12 & a13 & a14 & a15 & a16 & a17 \\ a21 & a22 & a23 & a24 & a25 & a26 & a27 \\ a31 & a32 & a33 & a34 & a35 & a36 & a37 \\ 0 & 0 & 0 & -\lambda_s & a45 & a46 & a47 \\ 0 & 0 & 0 & 0 & -\lambda_p & 0 & 0 \\ 0 & 0 & 0 & 0 & 0 & -\lambda_q & 0 \\ 0 & 0 & 0 & 0 & 0 & 0 & -\lambda_r \end{bmatrix}$$

$$\tilde{B}(\tilde{x}) = \begin{bmatrix} 0 & 0 & 0 \\ 0 & 0 & 0 \\ 0 & 0 & 0 \\ 0 & 0 & 0 \\ 1 & 0 & 0 \\ 0 & 1 & 0 \\ 0 & 0 & 1 \end{bmatrix}$$

where

$$a11 = \frac{\bar{q}Sd^2}{2I_xV}C_{l_p}\cos\alpha$$

$$a12 = \alpha_1\frac{I_y - I_z}{I_x}r$$

$$a13 = (1-\alpha_1)\frac{I_y - I_z}{I_x}q - \frac{\bar{q}Sd^2}{2I_xV}C_{n_r}\sin\alpha$$

$$a14 = \frac{\bar{q}Sd}{sI_x}(C_{l_0}\cos\alpha - C_{n_0}\sin\alpha)$$

$$a15 = \frac{\bar{q}Sd}{I_x}(C_{l_{\delta p}}\cos\alpha - C_{n_{\delta p}}\sin\alpha)\frac{\text{satsin}(30,\widetilde{\delta p})}{\widetilde{\delta p}}$$

$$a16 = -\frac{\bar{q}Sd}{I_x}(C_{l_{\delta q}}*\cos\alpha - C_{n_{\delta q}}\sin\alpha)\frac{\text{satsin}(30,\widetilde{\delta q})}{\widetilde{\delta q}}$$

$$a17 = -\frac{\bar{q}Sd}{I_x}(C_{l_{\delta r}}*\cos\alpha - C_{n_{\delta r}}\sin\alpha)\frac{\text{satsin}(30,\widetilde{\delta r})}{\widetilde{\delta r}}$$

$$a21 = \alpha_2\frac{I_z - I_x}{I_y}r$$

$$a22 = \frac{\bar{q}Sd^2}{2I_yV}*C_{m_q}$$

$$a23 = (1-\alpha_2)\frac{I_z - I_x}{I_y}p$$

$$a24 = \frac{\bar{q}Sd}{sI_y}C_{m_0}$$

$$a25 = \frac{\bar{q}Sd}{I_y}C_{m_{\delta p}}\frac{\text{satsin}(30,\widetilde{\delta p})}{\widetilde{\delta p}}$$

$$a26 = -\frac{\bar{q}Sd}{I_y}C_{m_{\delta q}}\frac{\text{satsin}(30,\widetilde{\delta q})}{\widetilde{\delta q}}$$

$$a27 = -\frac{\bar{q}Sd}{I_y}C_{m_{\delta r}}\frac{\text{satsin}(30,\widetilde{\delta r})}{\widetilde{\delta r}}$$

$$a31 = \alpha_3\frac{I_x - I_y}{I_z}q + \frac{\bar{q}Sd^2}{2I_xV}C_{l_p}\sin\alpha$$

$$a32 = (1-\alpha_3)\frac{I_x - I_y}{I_z}p$$

$$a33 = \frac{\bar{q}Sd^2}{2I_zV}C_{n_r}\cos\alpha$$

$$a34 = \frac{\bar{q}Sd}{sI_z}(C_{l_0}\sin\alpha + C_{n_0}\cos\alpha)$$

$$a35 = \frac{\bar{q}Sd}{I_z}(C_{l_{\delta p}}\sin\alpha + C_{n_{\delta p}}\cos\alpha)\frac{\text{satsin}(30,\widetilde{\delta p})}{\widetilde{\delta p}}$$

$$a36 = -\frac{\bar{q}Sd}{I_z}(C_{l_{\delta q}}\sin\alpha + C_{n_{\delta q}}\cos\alpha)\frac{\text{satsin}(30,\widetilde{\delta q})}{\widetilde{\delta q}}$$

$$a37 = -\frac{\bar{q}Sd}{I_z}(C_{l_{\delta r}}\sin\alpha + C_{n_{\delta r}}\cos\alpha)\frac{\text{satsin}(30,\widetilde{\delta r})}{\widetilde{\delta r}}$$

Presently, the α_i's have been selected as

$$\alpha_1 = \alpha_2 = \alpha_3 = .5$$

11